International Journal of Greenhouse Gas Control xxx (2013) xxx–xxx

Contents lists available at SciVerse ScienceDirect

International Journal of Greenhouse Gas Control

journal homepage: www.elsevier.com/locate/ijggc

Electrical resistance tomographic monitoring of CO_2 movement in deep geologic reservoirs

Charles R. Carrigan[a,*], Xianjin Yang[a], Douglas J. LaBrecque[b], Dennis Larsen[c], David Freeman[d], Abelardo L. Ramirez[a], William Daily[b], Roger Aines[a], Robin Newmark[e], Julio Friedmann[a], Susan Hovorka[f]

[a] Lawrence Livermore National Laboratory, 7000 East Avenue, Livermore, CA 94550, United States
[b] Multi-Phase Technologies, Sparks, NV 89431, United States
[c] Promore Industries (Core Lab), 6510 West Sam Houston Parkway N, Houston, TX 77041, United States
[d] Sandia Technologies, Houston, TX, United States
[e] National Renewable Energy Laboratory, Golden, CO 80401, United States
[f] Bureau of Economic Geology, University of Texas, Austin, TX 78758, United States

ARTICLE INFO

Article history:
Received 4 February 2013
Received in revised form 15 April 2013
Accepted 16 April 2013
Available online xxx

Keywords:
Electrical resistance tomography
Electrical resistivity
CO_2 saturation
Monitoring of carbon sequestration
Deep geologic reservoir
Cranfield field test

ABSTRACT

Deep geologic sequestration of carbon dioxide (CO_2) is being evaluated internationally to mitigate the impact of greenhouse gases produced during oil- and coal-based energy generation and manufacturing. Natural gas producing fields are particularly attractive sites for sequestration activities owing to the assumption that the same geologic barrier or cap rock permitting the subsurface regime to act as a long term natural gas reservoir will also serve to permanently contain the injected supercritical CO_2. Electrical resistance tomography (ERT) can potentially track the movement and concentration of the injectate as well as the degree of geologic containment using time lapse electrical resistivity changes resulting from injecting the super-critical fluid into the reservoir formation. An experimental cross-well ERT system operated successfully for more than one year obtaining time lapse electrical resistivity images during the injection of approximately one-million tons of CO_2 at a depth exceeding 3000 m in an oil and gas field in Cranfield, MS, representing the deepest application of the method to date. When converted to CO_2 saturation, the resultant images provide information about the movement of the injected CO_2 within a complex geologic formation and the development of the saturation distribution with time. ERT demonstrated significant potential for near real-time assessment of the degree of geologic containment and for updating risk analyses of the sequestration process. Furthermore, electrical resistivity imaging of the developing CO_2 distribution may provide crucial input about the developing reservoir pressure field that is required for active reservoir management to prevent the occurrence of cap-rock-damaging seismic activity.

1. Introduction

Deep sequestration of carbon dioxide within the Earth is actively being considered as one geo-engineering approach to reduce the atmospheric build-up of this greenhouse gas as a result of burning fossil fuels by industry and power utilities. Major sequestration projects are being undertaken in a number of countries including Canada (Weyburn-Midale), Germany (CO2 Sink), Norway (Sleipner), North Africa (In Salah) and the United States. The US Department of Energy sponsored Southeast Regional Carbon Sequestration Partnership (SECARB) Cranfield project near Natchez, Mississippi has become the fifth worldwide and the first in the US to inject more than a million tons of CO_2 into the subsurface (Jacobs, 2009). The geologic sequestration process typically involves extracting CO_2 from a combustion or production process, conversion to a liquefied or super-critical state ($T \geq T_c = 31.1\,^{\circ}C$, $P \geq P_c = 7.39$ MPa) involving one or more stages of compression, transport via pipeline to the deposition site followed by deep injection into a permeable subsurface regime that in the case of the Cranfield project is the Lower Tuscaloosa formation. Centered at a depth of about 3150 m, the injection zone consists predominantly of interbedded sandstone layers supporting a saline aquifer. This approximately 25 m thick sequestration reservoir is bounded above and below by low permeability mudstone. Maintaining the overall

* Corresponding author at: P.O. Box 808, L-052, Livermore, CA 94551, United States. Tel.: +1 925 422 3941; fax: +1 925 423 4077.
E-mail addresses: carrigan1@llnl.gov (C.R. Carrigan), xianjin.yang@gmail.com (X. Yang).

1750-5836/$ – see front matter © 2013 Elsevier Ltd. All rights reserved.
http://dx.doi.org/10.1016/j.ijggc.2013.04.016

integrity of the upper boundary or cap is critical to the concept of geologic sequestration as failure to do so may result in contamination of overlying or adjacent freshwater aquifers as well as the potential release of CO_2 at the surface.

Indeed, current discussions in the carbon capture and sequestration community have focused on the potential for injection-induced changes in the local stress field of a sequestration reservoir giving rise to hydrofractures or faulting in the cap rock with subsequent leakage into overlying fresh water aquifers or to the surface (Zoback and Gorelick, 2012). Continuous monitoring of temporal changes in the saturation of large volumes of CO_2 in the subsurface also has application for evaluating the storage characteristics of a formation as well as the interaction of the contained fluid with its porous reservoir including flow-path-modifying processes such as long-term CO_2-induced mineral dissolution or deposition.

Electrical resistance tomography (ERT) is an indirect method for visualizing the movement of fluids in porous media requiring the intermediate application of inversion algorithms that convert raw measurements of electrical resistance to a tomographic image (resistivity or concentration) of a fluid plume. The method assumes that detectable electrical resistivity changes in the permeable monitoring zone accompany the invasion of the fluid, here super critical CO_2, which is characterized by an electrical resistivity that is significantly higher than that of saline pore fluids already resident in the porous medium. The technique involves passing a known electric current (DC) across a target zone while measuring the electric potential at a number of locations around the zone. Repeating this operation for a number of different current pathways through the zone creates a data set of resistance that can be inverted to produce the spatial distribution of resistivity consistent with the potentials resulting from the applied currents. Electrodes for passing currents and measuring potentials are usually evenly spaced along boreholes and sometimes across the surface defining the boundaries of the target zone. Previous applications of geophysical ERT have involved mainly shallow (10–50 m) imaging of plumes in the vadose zone simulating infiltration from the surface (Daily et al., 1992; Carrigan, 2000) or imaging of steam fronts (~300 m depth) during enhanced oil recovery operations (Daily et al., 2004). The first major application of tracking CO_2 plumes following injection into a sequestration reservoir was performed in Ketzin, Germany as part of the ongoing CO_2 Sink Project (~650 m) (Kiessling et al., 2010; Schmidt-Hattenberger et al., 2011).

The Cranfield experiment involves imaging plumes at a depth of 3200 m (2.0 miles), the deepest application of ERT to date. Because the cabling and electrodes for the system were entirely mounted on the outside of the borehole casing, the system had to be designed to potentially withstand significant abrasion caused by contact with the borehole wall during installation. At the depth of emplacement, high temperatures and fluid pressures posed significant and sometimes competing challenges to the design of a sufficiently armored and electrically insulated borehole ERT system. The very long runs of borehole cable connecting the electrodes to the surface also created concerns that interfering electric currents could be induced in the system by other instrumentation as well as low frequency, solar-wind induced magnetotelluric fluctuations. Finally, the boreholes were not dedicated to the operation of the cross well ERT system alone as seismic, fluid sampling, pressure and thermal sensing instrumentation was also present in the monitoring boreholes which required significant compromises in design (Hovorka et al., 2013).

For the novel ERT application at Cranfield, assessing the feasibility of applying the technique to visualize CO_2 injection in a target zone at a depth of 3200 m was the main objective and challenge of this work given the high risk of failure. Assuming useful data could be acquired from the cross-well ERT system once installed, a secondary objective was to produce interpretable images of the CO_2 plume development that could be compared/combined with the results of borehole monitoring techniques and a cross well seismic system that unfortunately failed before injection began.

2. Experiment design

2.1. Site description

The Cranfield site is located about 16 miles east of Natchez, Mississippi (Fig. 1 of Hovorka et al., 2013) and it is an oilfield that operated originally between 1943 and 1966 followed by quiescence until 2008 when enhanced oil recovery operations involving CO_2 injection were initiated. At depths greater than 3000 m, the 20–28 m thick fluvial Lower Tuscaloosa sandstone injection zone effectively bounds CO_2 movement across its periphery by the four-way anticline of the layering as well as vertically by the presence of low-permeability mudstone layers above and below the injection zone (Hovorka et al., 2013). The injection zone itself appears to consist of braided stream channels and valleys filled with high-permeability interbedded sandstones and conglomerates (Kordi et al., 2010). The meandering nature of the channels and valleys introduces out-of-plane flows in the 2-D cross-well ERT imaging that can potentially complicate its interpretation as will be discussed. Between the injection zone and the surface, a number of high-transmissivity sandstones alternate with the cap-like fine grained layers and should act as buffers to attenuate any upward migration of the injectate in the event of leakage from the reservoir (Chabora and Benson, 2009).

2.2. ERT system design and installation

Fig. 1 illustrates the relationship between the injection well and the two monitoring boreholes that provided access to the injection zone for the cross well ERT system. In the collinear arrangement shown, the closest monitoring well (F2) to the injection well is about 70 m (270 ft) distant while the F2 and F3 monitoring wells themselves were separated by about 33 m (106 ft). Because the electrodes and the target formation must be electrically insulated from the well casing to prevent short circuiting of the transmitted currents along the boreholes, approximately 130 m (400 ft) of non-conductive fiberglass well casing was used in each monitoring well to span the injection zone and adjacent impermeable zones. In F2, a vertical array of 14 electrodes with 4.6 m (15 ft) spacing and 61 m (195 ft) total length was centered on the injection zone while in F3 only 7 electrodes spanned the same array length requiring an increase in spacing to 9.14 m (30 ft), the difference in electrode spacing being entirely the result of cost considerations.

In system design, we focused on development challenges specifically related to (1) deep emplacement (10,000 ft or 3280 m) and (2) minimizing physical and electrical interference between ERT and other monitoring methods operating in the same well. Besides requiring very long runs of electrical cable (over 2 miles) that potentially can induce a noise current due to the operation of nearby equipment as well as fluctuations in the magnetotelluric field, the ERT target zone was characterized by temperatures in excess of 120 °C (250 F), fluid pressures exceeding 34 MPa (5000 psi) and highly acidic saline ground water (pH ~3–4). While ERT system components (electrodes and cabling) tend to be rather rugged compared to other types of sensors (e.g., seismic, pressure gauge), the system design was still required to take into account the deleterious effects of temperature, pressure and ground water chemistry as data acquisition was anticipated to occur during the year following installation. Another challenge specific to the Cranfield application is that the ERT system was mounted externally on the well casing

Please cite this article in press as: Carrigan, C.R., et al., Electrical resistance tomographic monitoring of CO_2 movement in deep geologic reservoirs. Int. J. Greenhouse Gas Control (2013), http://dx.doi.org/10.1016/j.ijggc.2013.04.016

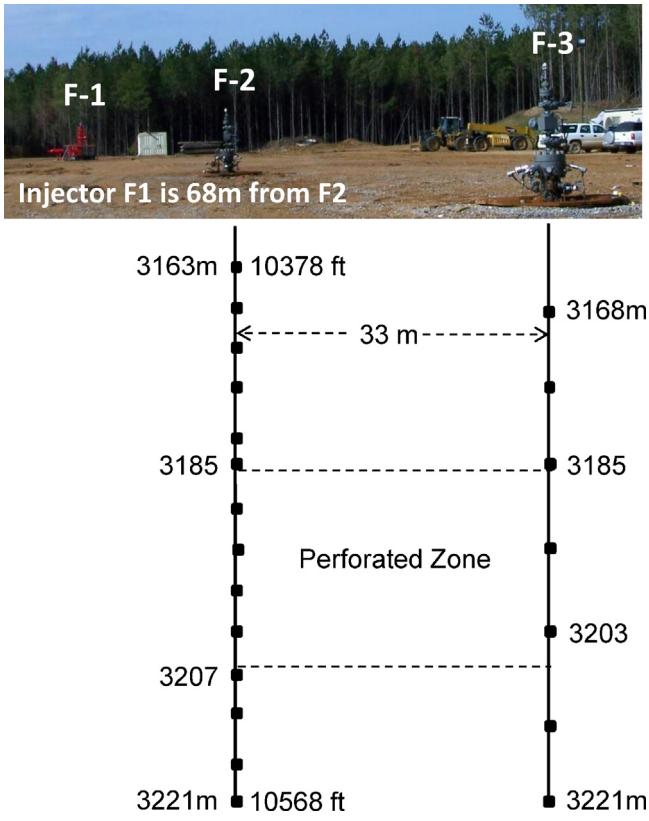

Fig. 1. Layout of one injection well F1 and two monitoring wells F2 and F3. There are 14 electrodes in F2 and 7 electrodes in F3.

and subjected to a very long run in an open hole. While ERT systems are conventionally mounted on the outside of a plastic (PVC), non-conductive casing, the insertion depths have been very much shallower in previous installations. Because of the very long runs of exposed borehole wall in the Cranfield case, a very high probability existed that non-uniformities in the open-borehole wall would lead to binding or snagging of the cabling system as it is lowered down the well on the casing. Furthermore, if the hole is not straight or vertical during the casing insertion, which is not unusual for a 2-mile deep well, the weight of the casing can potentially ride on the cabling causing abrasion or even breakage if enough centralizers are not used. Once the system reaches the bottom of the borehole, the well is grouted in. This involves pumping cement down the well and up the annulus formed by the casing and borehole wall. This activity represents yet another possibility for abrasion of the exterior-mounted cabling and components.

The Cranfield ERT system was designed to minimize the potential for deployment failure, making use of non-conductive borehole centralizers and stainless steel tubes individually encapsulating each of the conductors connecting an electrode to the surface. However, use of conductive steel tubing to mechanically protect the contained electrical wires also introduced the possibility that any moisture penetrating the system could produce current leakage by transmission along the protecting tubes to the environment. In addition to the damaging effect of unknown stray electric currents on the imaging process, current leakage to the steel tubing can produce "cross talk" between the ideally high-impedance channels of the ERT system. However, the system was designed so that minor mechanical damage resulting in moisture leakage at one or more points in the system would not necessarily introduce sufficient stray currents or cross talk to prevent the acquisition of some useful data from the electrode array.

Fig. 2a shows the L-316 stainless steel electrodes mounted on the fiberglass casing with their epoxy-based centralizers. The stainless electrodes were used as a compromise between longevity in a corrosive environment and minimizing the level of electrical noise in the system. Individual steel-tubing encapsulated cables were connected to each electrode and run upward along the casing to a custom-designed splitter (Fig. 2b) that provided the transition from either 7 or 14 individually armored cables to either one (F3) or two (F2) 7-conductor wireline cables. The wireline cables were continued another 3000 m to the surface where they were connected to a Multi-Phase Technologies DAS-1 Electrical Impedance Tomography System®. The system combines transmitter, receivers, and a multiplexer that monitors up to 64 electrodes and can be programmed to transmit currents and perform simultaneous voltage measurements on pre-determined sets of electrodes according to any given monitoring schedule. Once installed, the system is entirely automated and allows downloading of data sets and modifications of the ERT sampling schedules remotely over the Internet.

2.3. ERT monitoring approach

Measurements of electric potential between electrode pairs are performed using a DC 4-electrode measurement approach; a constant electric current is transmitted between two selected electrodes while potential differences are measured between certain pairs of the remaining electrodes. During operation of the ERT system at Cranfield, approximately 10,000 potential measurements were made daily using 4-different electrode sampling schedules for a period of more than one year following CO_2 injection. In addition to reciprocal measurements for each data set, multiple data sets were obtained every day of operation. This oversampling strategy facilitates data quality assurance and leaves room for removal of noisy data. The data sets were downloaded from the Internet and used in an inversion program.

Following installation of the cross well system and before injection was initiated, multiple ERT data sets were obtained to evaluate the natural background resistivity distribution. This is an important element of the monitoring approach because such measurements provide a baseline or reference resistivity distribution for comparison with measurements obtained following the start of injection. At Cranfield, the baseline measurements started approximately 5 days before injection with a number of data sets being obtained to construct a reference data set.

3. ERT data processing methods

ERT data processing includes three primary steps: preprocessing for identification and removal of noisy data points with multiple thresholds and time series analysis, assembly and inversion of a baseline data set, and then difference inversion of daily monitoring data sets for resistivity distribution that was converted to CO_2 saturation.

3.1. Preprocessing

To prepare ERT data for time lapse inversion, we identified and removed noisy data that may result in inversion artifacts. The noisy data consist of inaccurate measurements due to imperfect equipment and outliers caused by subsurface events other than CO_2 injection.

Inaccurate measurements were removed based on several thresholds: minimum measured voltage (10 μV), minimum injected current (10 mA), minimum resistance (50 μΩ), maximum contact resistance (500 Ω) and maximum reciprocal measurement error (10%). A robust data error estimate can be obtained by

Please cite this article in press as: Carrigan, C.R., et al., Electrical resistance tomographic monitoring of CO_2 movement in deep geologic reservoirs. Int. J. Greenhouse Gas Control (2013), http://dx.doi.org/10.1016/j.ijggc.2013.04.016

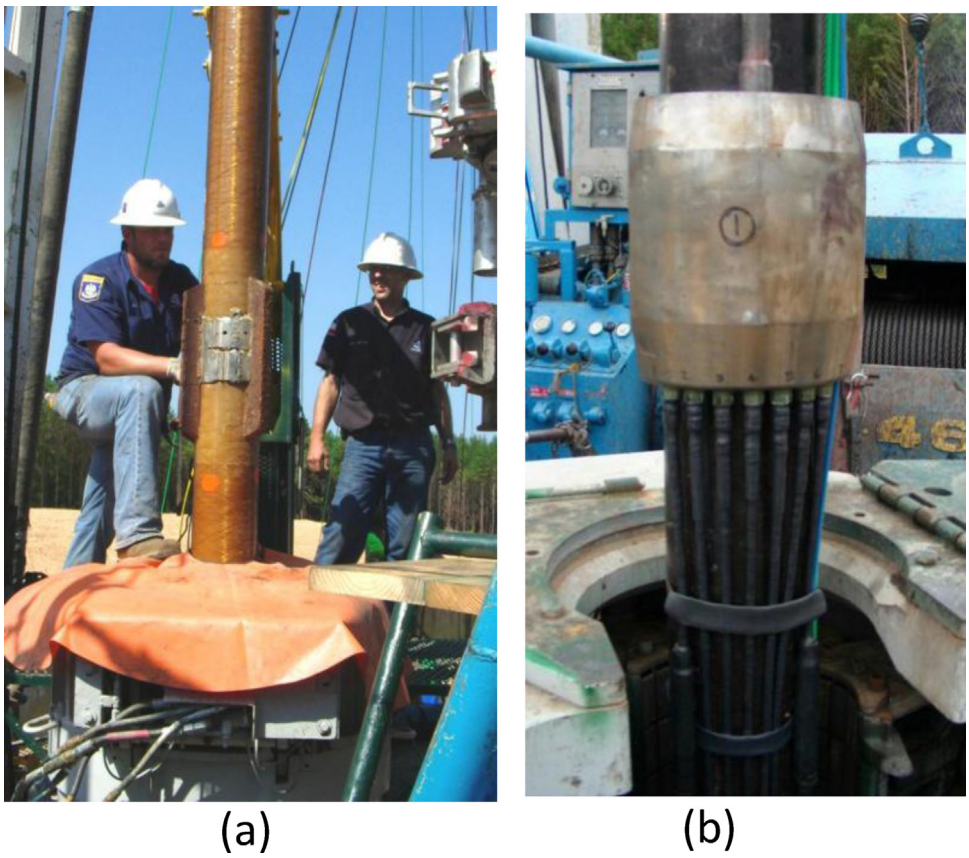

Fig. 2. (a) ERT electrode band, mounted on non-conductive casing, is prepared for installation. Electrodes are protected by non-conductive, epoxy-based centralizers. (b) Splitter resides above electrode array and combines electrode cables (either 14 or 7) into either two or one 7-conductor wireline cables which are continued to surface.

comparing reciprocal measurements obtained by switching transmitting and receiving electrode bipoles. The resistance of reciprocal measurements should be identical according to the Lorentz reciprocity theorem of electromagnetism. If a reciprocal error is above the 10% threshold, both forward and reciprocal measurements are removed. If the reciprocal error is less than the threshold, forward and reverse measurements are averaged to form one data point. The reciprocal error was then used as the data weight in the inversion. Fig. 3 summarizes the noise level of our data. The vertical axis is the fractional amount of data residing in a particular Reciprocal Error bin. About 60.6% of reciprocal measurements had less than 10% reciprocal error. Almost 40% of reciprocal data with more than 10% reciprocal error indicates a noisy downhole environment.

After threshold-based preprocessing that left more accurate data, we took an average of multiple (1–4) repeat data sets that were collected on the same day. A data point was considered noisy for removal if repeat measurements on the same day varied over 10%. This daily averaging process removed more outliers, further improved data quality and ended up with one data set per day.

In our last preprocessing step we used a time series analysis method to identify and remove data outliers that were not likely to be created by CO_2 injection. We conducted time series analysis for measurements taken with the same transmitting and receiving electrodes on different days. The time series analysis was based on the assumption that both the short term changes of resistance induced by CO_2 injection in a few days and long term changes in a few months were bounded and varying smoothly in time. Our synthetic data tests with a layered earth model indicated that typical CO_2 saturation changes at Cranfield may result in maximum 5% daily change of resistance. Fig. 4 shows typical acceptable resistances change from day to day. But Fig. 5 is an example of

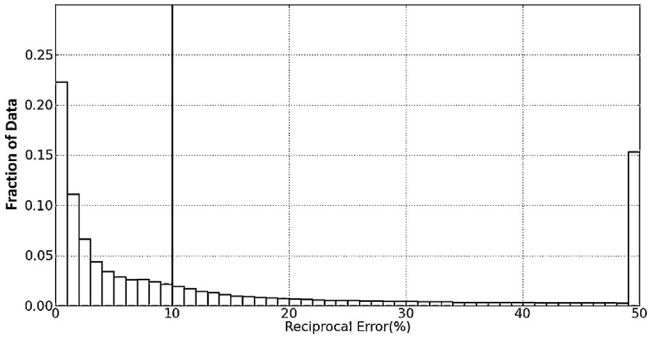

Fig. 3. Histogram of reciprocal errors for ERT data from 11/29/2009 to 3/12/2010. The vertical line indicates the 10% reciprocal error threshold. The huge spike at the end accounts for data with a reciprocal error equal to or greater than 50%.

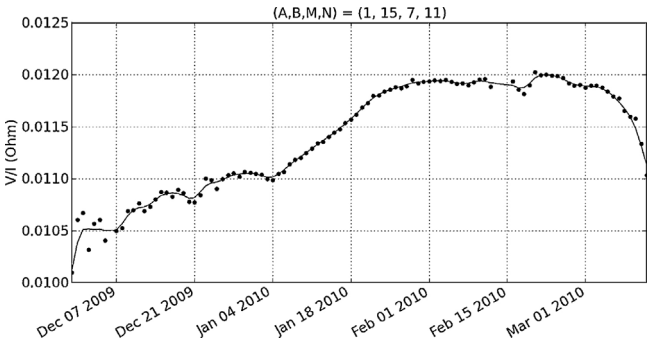

Fig. 4. An acceptable time series for electrode sequence (A, B, M, N) = (1, 15, 7, 11).

Please cite this article in press as: Carrigan, C.R., et al., Electrical resistance tomographic monitoring of CO_2 movement in deep geologic reservoirs. Int. J. Greenhouse Gas Control (2013), http://dx.doi.org/10.1016/j.ijggc.2013.04.016

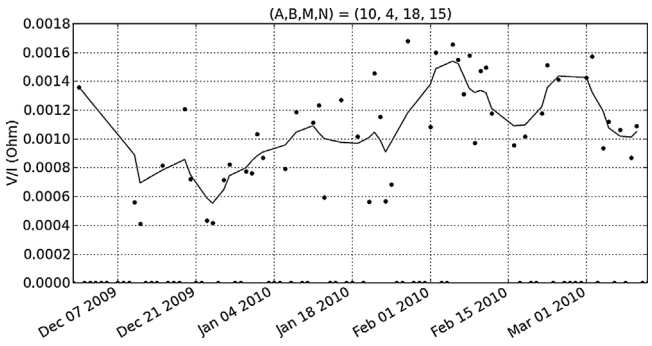

Fig. 5. An unacceptable time series for electrode sequence (A, B, M, N) = (10, 4, 18, 15) with a large oscillation of electrical resistance from day to day.

unacceptable time series of electrical resistance. A and B in Figs. 4 and 5 indicate two transmitting electrodes, and M and N are two receiving electrodes. Four numbers such as (1, 15, 7, 11) in parenthesis are four electrode identifiers among 21 installed electrodes. The round dots are actual measurements and the line is a smoothed trend. Time series analysis helped remove some electrode configurations that produced irregular time series of electrical resistance.

Time series analysis also revealed that a large number of electrode configurations produced drastic and abrupt changes of resistance after March 12, 2010. We were unable to determine the cause of these large rapid changes, so we limited our analysis of data sets collected before March 12, 2010.

It is important to point out that the input data for time-series analysis survived a gauntlet of powerful data filters. These data are all considered accurate measurements based on the various criteria we described earlier. This time series analysis identified data outliers incurred not by CO_2 saturation changes but by electrode and cable degradation or other unknown downhole events. After extensive removal of noisy data, the remaining usable data revealed that all 21 electrodes were involved in the data collection and there were no completely failed electrodes.

3.2. Baseline data preparation

The baseline data set was constructed from the average of five data sets collected between 11/29/2009 and 12/3/2009 before and slightly after CO_2 injection began on 12/1/2009. The data collected on 12/3/2009 should be free from the influence of injected CO_2 because the initial CO_2 breakthrough in the monitoring well F2 occurred on 12/12/2009. A mean and standard deviation of five data sets were calculated and we used the coefficient of variation (CV), the ratio of standard deviation to the mean, as a threshold to remove individual noisy data points. A data point with a CV value larger than 0.1 was rejected. Inversion of baseline data produces a reference model for time lapse inversion to compare with subsequent data sets. It is crucial to have a less noisy baseline data set.

3.3. Difference inversion

For time lapse data inversion we used an in-house three-dimensional (3D) ERT inversion program that was adapted from LaBrecque et al. (1999) and LaBrecque and Yang (2001). In the forward problem, the governing partial differential equation of electric fields was converted to linear equations with the finite difference method (Dey and Morrison, 1979). The linear system was solved iteratively using the preconditioned conjugate gradient method with a symmetric successive over-relaxation (SSOR) preconditioner (Spitzer, 1995). A smooth-model least-squares inverse algorithm minimizes the sum of weighted data misfit and model roughness. This process results in a smooth model whose forward solution best fits measured data to a predetermined noise level. For noisy data sets, a robust reweighting scheme was used to down-weight poorly fit data from iteration to iteration (LaBrecque et al., 1999).

The time lapse monitoring data sets were inverted using the difference inversion algorithm described by LaBrecque and Yang (2001). The difference inversion method inverts the difference between monitor and baseline data sets and uses the baseline resistivity model as the a priori model. A monitoring data set is compared with the baseline data set and only the matching data points are used in the difference inversion. The primary advantage of this method is that the effects of systematic and coherent data noise are mitigated so that fewer inversion artifacts are shown on the difference images.

3.4. Resistivity to CO_2 saturation

CO_2 saturation can be estimated from resistivity data by substituting saline fluids with insulating CO_2 in the Archie's equation:

$$\rho = \frac{a \cdot \phi^{-m} \cdot \rho_w}{S_w^n} \quad (1)$$

where ρ is the bulk resistivity of the rock, ρ_w is the resistivity of the brine, ϕ is the porosity of the formation, S_w is the brine saturation, n is the saturation exponent, a and m are empirical parameters that will be cancelled in our derivation below. For time lapse monitoring of a deep reservoir, the baseline brine saturation before CO_2 injection is 100%, i.e.,

$$\rho_0 = a \cdot \phi^{-m} \cdot \rho_w \quad (2)$$

Divide Eq. (1) by Eq. (2), note that $S_w + S_{CO_2} = 100\%$, and solve for S_{CO_2} (Naktsuka et al., 2010).

$$S_{CO_2} = 1 - \left(\frac{\rho_0}{\rho}\right)^{1/n} \quad (3)$$

Eq. (3) indicates that CO_2 saturation can be estimated from the ratio of monitored resistivity to the baseline resistivity. The saturation exponent n is set to 2.0, a widely used default value.

4. Monitoring results

The baseline data collected before CO_2 injection began on December 1, 2009 was inverted using an iteratively reweighted least squares smooth model inversion method (LaBrecque et al., 1999). Ninety monitor data sets from 12/10/2009 to 3/12/2010 were then inverted using the difference inversion method. Percent resistivity changes between monitor and baseline resistivity models were converted to CO_2 saturation. The images in Fig. 6 show time lapse CO_2 saturation changes related to arrival and growth of the CO_2 plume in the imaging zone. It is clear that (1) the saturation images have very few artifacts after thorough data cleanup; (2) most saturation changes occurred within the more permeable reservoir layer; (3) CO_2 saturation increases with time and (4) CO_2 plumes are continuous and grow consistently.

Fig. 7 illustrates plume development between F2 and F3 out to more than 100 days. Again, the plume development is continuous and grows in strength with time. The heterogeneous nature of the formation is apparent as the plume develops. Interestingly, the flow paths are not constant but seem to evolve as filling of the target zone occurs which may be a result of the movement of native pore fluids displaced by the CO_2.

The Schlumberger reservoir saturation tool (RST) was also used to obtain CO_2 saturation in the monitoring wells. Fig. 8 compares

Please cite this article in press as: Carrigan, C.R., et al., Electrical resistance tomographic monitoring of CO_2 movement in deep geologic reservoirs. Int. J. Greenhouse Gas Control (2013), http://dx.doi.org/10.1016/j.ijggc.2013.04.016

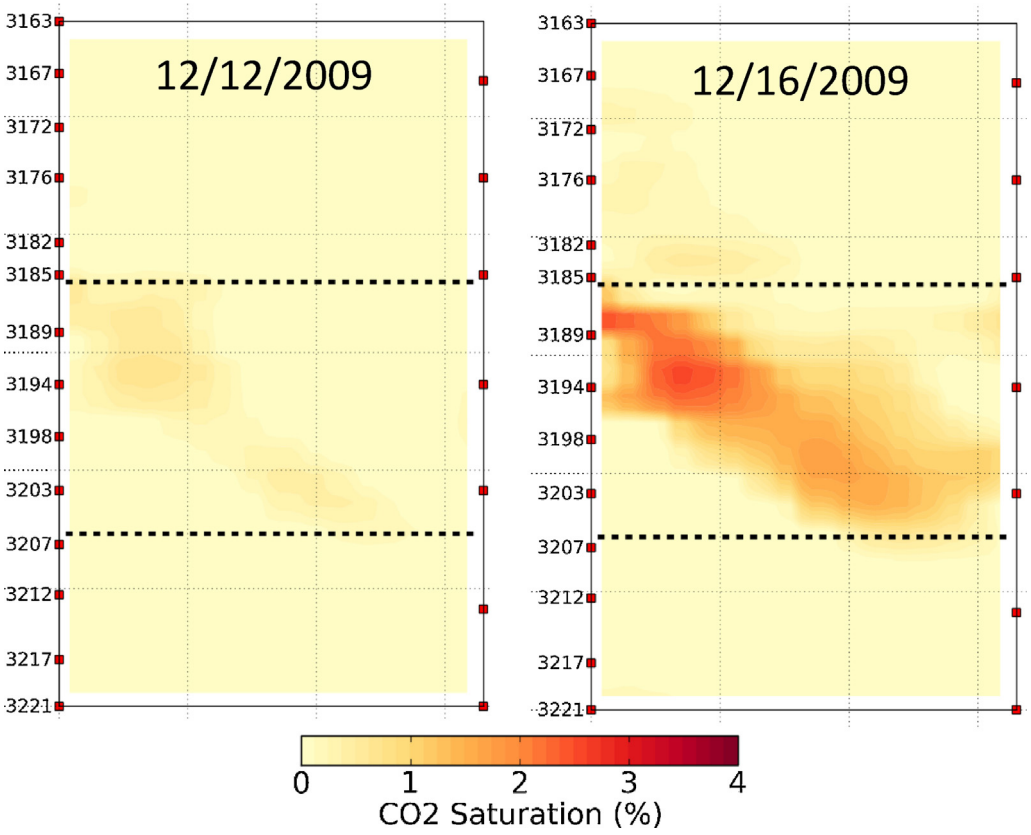

Fig. 6. CO_2 saturation images showing CO_2 breakthroughs in monitoring wells F2 (left) and F3 (right) after CO_2 injection began on 12/1/2009. Two dashed lines define approximate reservoir boundaries.

the CO_2 saturation in wells F2 and F3 from these two different methods. We noted some good spatial correlation between the two data sets although RST CO_2 saturation is clearly higher than ERT-derived CO_2 saturation. It is important to point out that RST is a point measurement tool that can "see" less than one foot (30 cm) and is very sensitive to the conditions around the borehole. However, ERT sensors provide an integrated response between the two monitoring wells that are 33 m apart and compared to the RST point measurements in the borehole, ERT has a relatively low maximum spatial resolution (3 m) at the Cranfield site due to the large electrode spacing (4.7 m in F2 and 9.4 m in F3). So CO_2 saturation obtained from ERT data is an average response from a large volume.

5. Discussion

The ERT method appears to be quite effective in capturing at least the lowest order characteristics of the CO_2 plume temporal evolution such as the arrival of the front at well F2 during 12–15 December, the appearance of the front at well F3 on about 16–17 December and the consistent outward expansion of the flow in a clearly heterogeneous layer as well as its confinement to the geologically determined impermeable zone. We find that the arrival times are in approximate agreement with first observations of CO_2 production at these wells according to the daily Cranfield operations log. Picking first arrivals is challenging for ERT because gas concentrations and hence resistivity contrasts will tend to be initially very low when the plume arrives at a well. Furthermore, volumetric averaging of the ERT signal will tend to reduce observed resistivity contrasts further. We find that ERT also captures the general spatial variations of CO_2 saturation near the F2 well as seen in Fig. 6. Again, the ERT saturation estimates are volumetrically averaged resistivity signals and small scale features, such as the distribution of CO_2 immediately adjacent to the well as determined by the RST method, will have underestimated saturations. While it is encouraging that the spatial variations are in general agreement, it is apparent that meaningful saturation values can only be obtained from plume features that are large compared to the averaging volume determined by the electrode spacing. In general, ERT estimates of plume dimensions were found to be quite comparable to those obtained from both the RST and crosswell acoustic inversion methods employed at Cranfield (see Table 2 of Hovorka et al., 2013). Imaging artifacts are inherent to the ERT inversion method owing mainly to noise and the underdetermined nature of the imaging problem. An additional source of imaging artifacts is the daily fluctuation of data coverage. The number of measurements used in the difference inversion from day to day varied from 434 to 460 with one outlier at 410 on February 16, 2010. This variation, though small, causes changes of ERT sensitivity that can result in imaging artifacts. Given this, the relatively low resolution of the imaging regime as a result of the sparse electrode spacing and noise introduced by damaged electrodes, it is surprising that so few persistent artifacts (e.g., those outside the impermeable zone) occur in the resistivity plots. The ability to minimize the occurrence of imaging artifacts suggests that ERT can be a useful monitoring tool for detecting persistent anomalies that may indicate CO_2 leakage into ideally gas-tight caprock.

6. Environmental implications

As a feasibility experiment, an automated cross-borehole ERT system was installed and operated continuously at a depth of more than 3000 m for more than one year following its emplacement at the SECARB Cranfield carbon sequestration site producing images of CO_2 plume evolution that appear to be reasonably correlated

Please cite this article in press as: Carrigan, C.R., et al., Electrical resistance tomographic monitoring of CO_2 movement in deep geologic reservoirs. Int. J. Greenhouse Gas Control (2013), http://dx.doi.org/10.1016/j.ijggc.2013.04.016

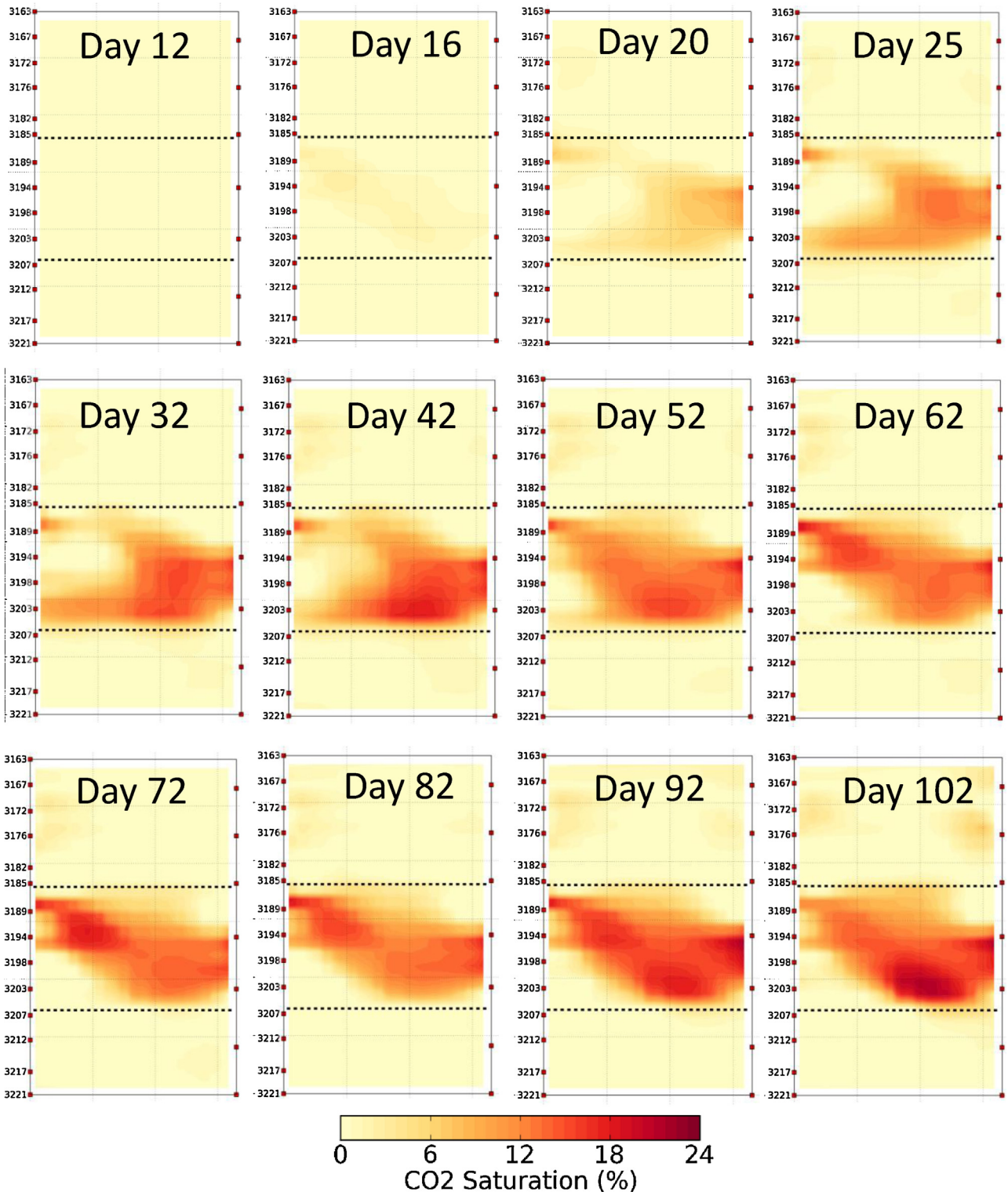

Fig. 7. Time lapse CO_2 saturation images for the first 102 days after CO_2 injection began on 12/1/2009. Two dashed lines define approximate reservoir boundaries.

with borehole observations and the known geology of the injection zone. This type of system has potential application to monitoring the flow and storage of injected CO_2 near the injection well for determining reservoir storage characteristics and chemically induced changes in flow paths. Given concerns about injection-induced fracturing of caprock, higher-resolution ERT may also have application as an "early-warning" system for the formation of fracture pathways in caprock that could result in environmental damage to overlying or nearby water resources. Another potential application involves monitoring the boundary of a sequestration lease to ensure that CO_2 does not migrate across the boundary to an adjacent parcel. This would require many boreholes for continuously monitoring the boundary of a large lease. Alternatively, boreholes could be located primarily along the path of greatest plume advancement. Because we have shown that very deep emplacement of the ERT system mounted on the outside

Please cite this article in press as: Carrigan, C.R., et al., Electrical resistance tomographic monitoring of CO_2 movement in deep geologic reservoirs. Int. J. Greenhouse Gas Control (2013), http://dx.doi.org/10.1016/j.ijggc.2013.04.016

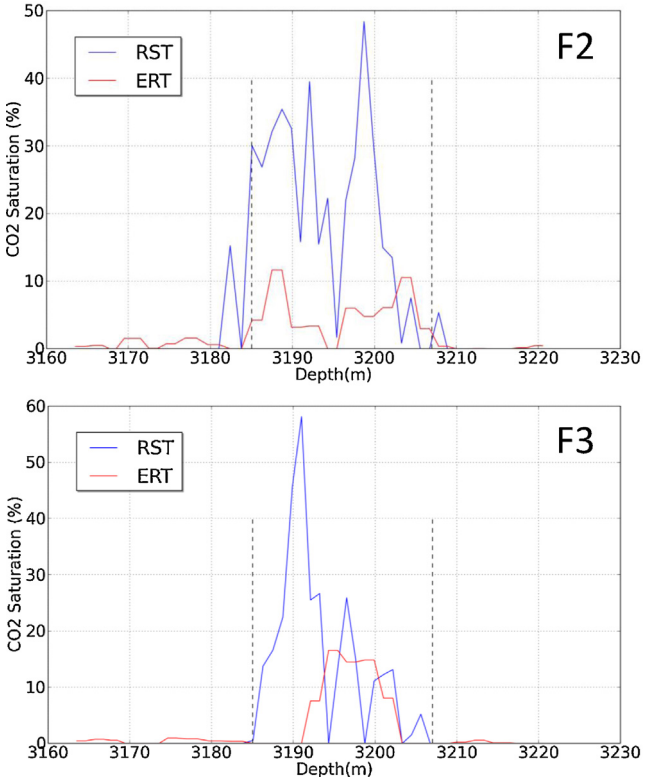

Fig. 8. Comparison of CO_2 saturations obtained from ERT and reservoir saturation tool (RST) in monitoring wells F2 and F3. The perforated zone for monitoring formation fluids is defined by the dashed lines.

of well casings is possible and that monitoring can occur in a multi-use environment, any ERT boreholes could also be used for other purposes which would effectively reduce the cost for monitoring.

Acknowledgments

Authors thank Robert J. Butsch of Schlumberger Carbon Services for providing electrode depth data based on his Array Induction Tool (AIT) logs. This ERT monitoring project was hosted by Southeast Regional Carbon Sequestration Partnership (SECARB), led by Southern States Energy Board, and funded by U.S. Department of Energy (DOE) National Energy Technology Laboratory (NETL; Bruce Brown, program manager) under Grant Number FC26-05NT42590. We also thank Denbury Onshore LLC for their support as the site host of this project. This work was performed under the auspices of the U.S. Department of Energy by Lawrence Livermore National Laboratory under Contract DE-AC52-07NA27344.

References

Carrigan, C.R., 2000. Understanding the fate and transport of multiphase fluid and colloidal contaminants in the vadose zone using an intermediate-scale field experiment. In: Looney, B., Falta, R. (Eds.), Vadose Zone, Science & Technology Solutions, vol. 2. Battelle Press, pp. 942–947.

Chabora, E.R., Benson, S.M., 2009. Brine displacement and leakage detection using pressure measurements in aquifers overlying CO_2 storage reservoirs. Energy Procedia 1, 2405–2412.

Daily, W., Ramirez, A.L., LaBrecque, D.J., Nitao, J., 1992. Electrical resistivity tomography of vadose water movement. Water Resources Research 28 (5), 1429–1442.

Daily, W., Ramirez, A., Newmark, R., Masica, K., 2004. Low-cost reservoir tomographs of electrical resistivity. The Leading Edge 23, 472–480.

Dey, A., Morrison, H.F., 1979. Resistivity modeling for arbitrarily shaped three-dimensional structures. Geophysics 44, 753–780.

Hovorka, S.D., Meckel, T.A., Trevino, R.H., 2013. Monitoring a large-volume injection at Cranfield, Mississippi – project design and recommendations. International Journal of Greenhouse Gas Control, http://dx.doi.org/10.1016/j.ijggc.2013.03.021 (in this issue).

Jacobs, M., 2009. DOE-Sponsored Mississippi Project Hits 1-Million-Ton Milestone for Injected CO_2. In: Fossil Energy Techline, DoE-FE, November 5.

Kiessling, D., Schmidt-Hattenberger, C., Schuett, H., Schilling, F., Krueger, K., Schoebel, B., Danckwardt, E., Kummerow, J., 2010. Geoelectrical methods for monitoring geological CO_2 storage: first results from cross-hole and surface-downhole measurements from the CO2SINK test site at Ketzin (Germany). International Journal of Greenhouse Gas Control 4 (2010), 816–826.

Kordi, M., Hovorka, S., Milliken, K., Treviño, R., Lu, J., 2010. Diagenesis and reservoir heterogeneity in the Lower Tuscaloosa Formation at Cranfield Field, Mississippi. GCCC Digital Publication Series #10–13.

LaBrecque, D.J., Morelli, G., Daily, W.D., Ramirez, A.L., Lundegard, P., 1999. Occam's inversion of 3-D ERT data. In: Oristaglio, M., Spies, B. (Eds.), Three-dimensional Electromagnetics, Geophysical Development No. 7, 575–590. Society of Exploration Geophysicists.

LaBrecque, D.J., Yang, X., 2001. Difference inversion of electrical resistivity tomography data – a fast inversion method for 3-D in-situ monitoring. Journal of Environmental and Engineering Geophysics 6 (2), 83–89.

Naktsuka, Y., Xue, Z., Garcia, H., Matsuoka, T., 2010. Experimental study on CO_2 monitoring and quantification of stored CO_2 in saline formations using resistivity measurements. International Journal of Greenhouse Gas Control 4 (2010), 209–216.

Schmidt-Hattenberger, C., Bergmann, P., Kießling, D., Krügera, K., Rücker, C., Schütt, H., Ketzin Group, 2011. Application of a vertical electrical resistivity array (VERA) for monitoring CO_2 migration at the Ketzin site: first performance evaluation. Energy Procedia 4, 3363–3370, http://dx.doi.org/10.1016/j.egypro.2011.02.258.

Spitzer, K., 1995. A 3-D finite difference algorithm for DC resistivity modeling using conjugate gradient methods. Geophysical Journal International 123, 903–914.

Zoback, M., Gorelick, B., 2012. Earthquake triggering and large-scale geologic storage of carbon dioxide. Proceedings of the National Academy of Sciences www.pnas.org/cgi/doi/10.1073/pnas.1202473109